

# Electronic Supplementary Material

## Adsorption performance and physicochemical mechanism of MnO<sub>2</sub>-polyethylenimine-tannic acid composites for the removal of Cu (II) and Cr(VI) from aqueous solution

Xiaoyan Deng<sup>1</sup>, Luxing Wang<sup>1</sup>, Qihui Xiu<sup>2</sup>, Ying Wang<sup>2</sup>, Hong Han<sup>2</sup>, Dongmei Dai<sup>2</sup>, Yongji Xu<sup>2</sup>, Hongtao Gao (✉)<sup>2</sup>, Xien Liu<sup>2</sup>

1 College of Environment and Safety Engineering, State Key Laboratory Base of Eco-Chemical Engineering, Qingdao University of Science & Technology, Qingdao 266042, China

2 College of Chemistry and Molecular Engineering, State Key Laboratory Base of Eco-Chemical Engineering, Qingdao University of Science & Technology, Qingdao 266042, China

E-mail: [gaohtao@qust.edu.cn](mailto:gaohtao@qust.edu.cn)

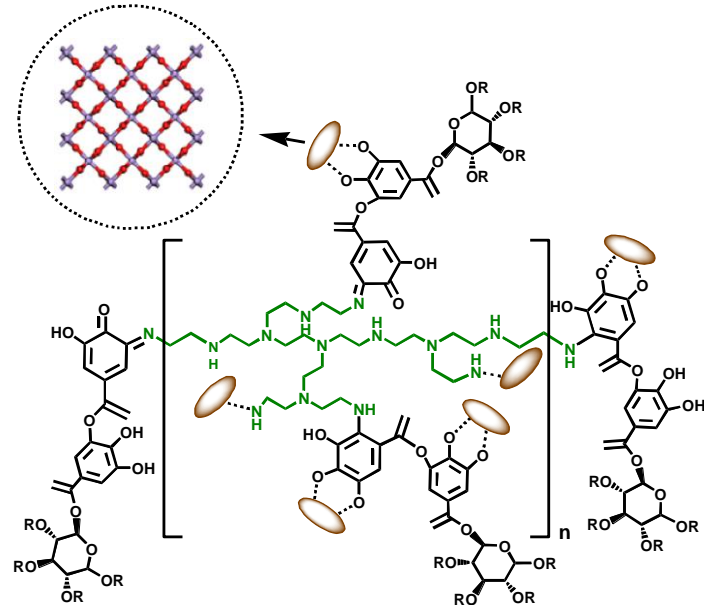


Fig. S1. Schematic graph of preparation of MnPT.

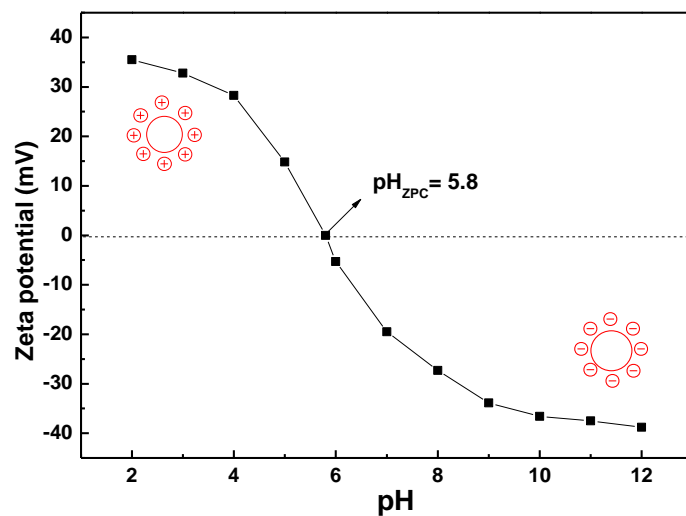


Fig.S2. Zeta potential of MnPT as a function of pH in 0.001 M  $\text{NaNO}_3$  electrolyte.

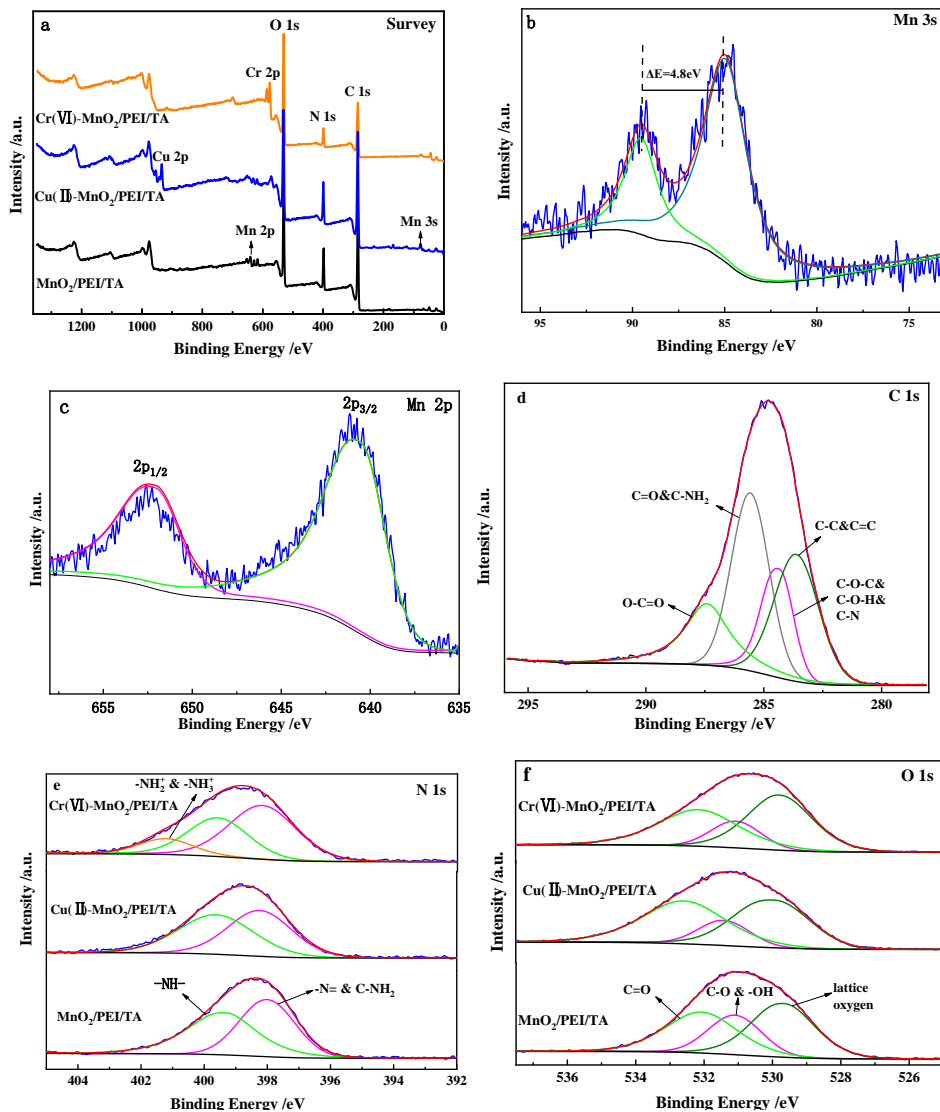


Fig. S3. (a) XPS survey spectra of samples. (b) Mn 3s, (c) Mn 2p, (d) C 1s, (e) N 1s and (f) O 1s high-resolution XPS spectra.

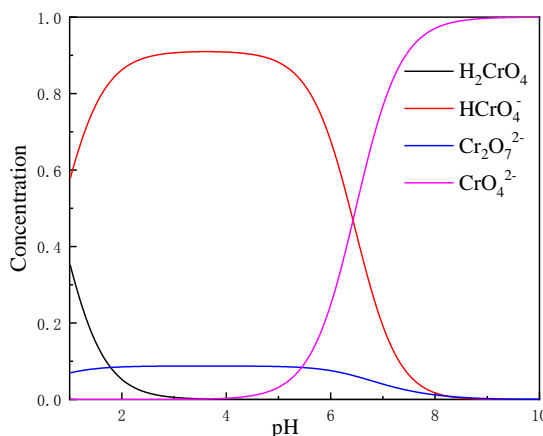


Fig. S4. The forms of Cr (VI) in aqueous solution with different pH.

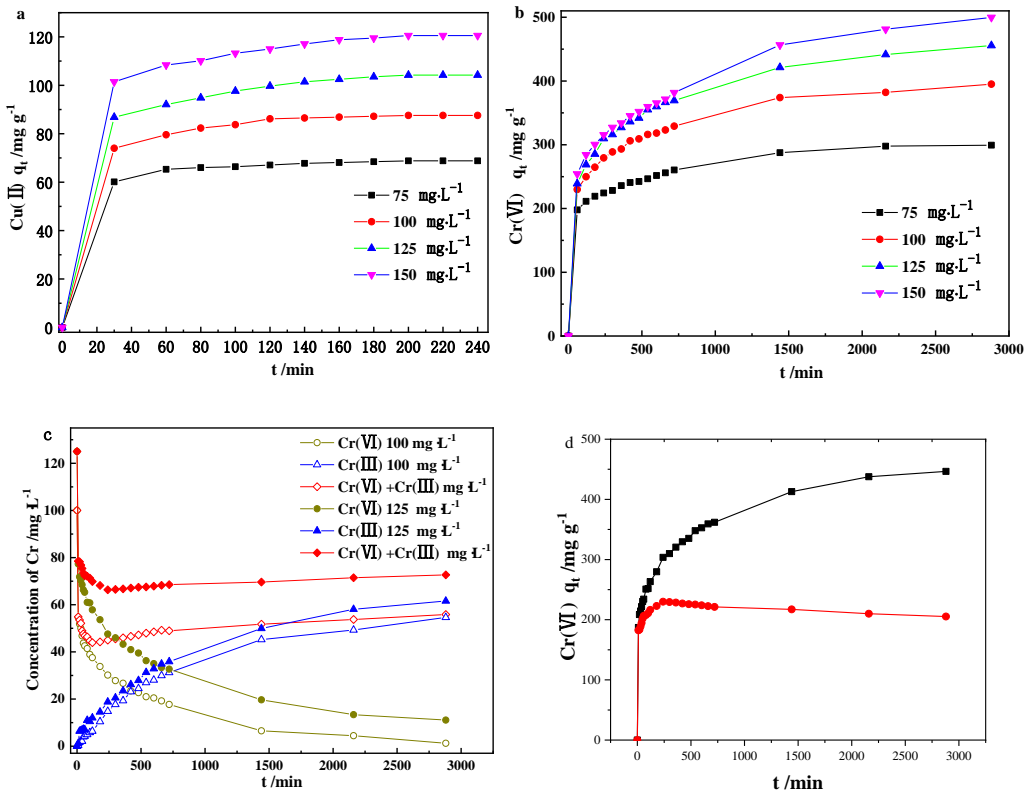


Fig. S5. Relationship between the removal capacity and time for the adsorption of Cu(II) (a) and Cr (VI) (b) by MnPT ( Cu(II):  $C_0 = 75 - 150 \text{ mg L}^{-1}$ ; MnPT =  $100 \text{ mg L}^{-1}$ ;  $T = 298\text{K}$ ; pH = 5.5; contact time = 4 h. Cr(VI):  $C_0 = 75 - 150 \text{ mg L}^{-1}$ ; MnPT =  $25 \text{ mg L}^{-1}$ ;  $T = 298\text{K}$ ; pH = 2.0; contact time = 48 h). (c) Variety of Cr with different valence states during the reaction (d) The removal capacity of Cr (VI) with concentration of  $125 \text{ mg L}^{-1}$  by MnPT through adsorption and redox reactions.

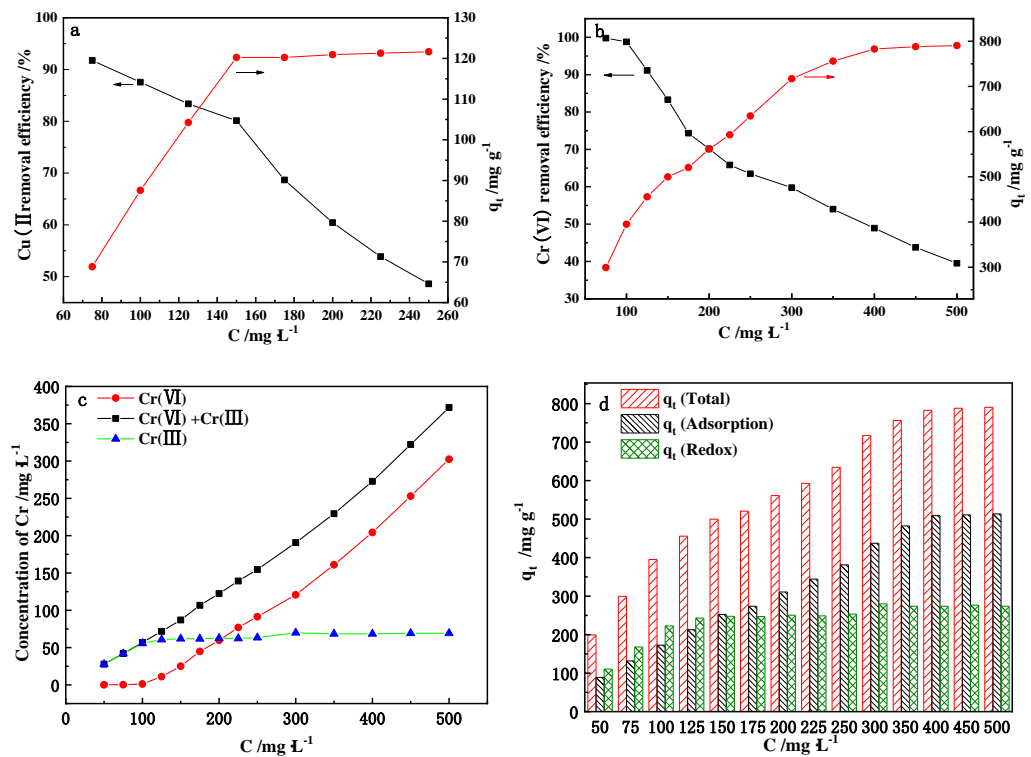


Fig.S6. Removal capacities with different initial concentrations of Cu(II) (a) and Cr(VI) (b) ( Cu(II):  $C_0 = 75 \sim 250 \text{ mg}\cdot\text{L}^{-1}$ ; MnPT = 100 mg·L<sup>-1</sup>; T = 298K; pH = 5.5; contact time = 4 h. Cr(VI):  $C_0 = 75 \sim 500 \text{ mg}\cdot\text{L}^{-1}$ ; MnPT = 25 mg·L<sup>-1</sup>; T = 298K; pH = 2.0; contact time = 48 h). (c) The concentration of Cr (III) and Cr (VI) remained in the solution after Cr (VI) removal experimental. (d) Cr (VI) removal capacity by MnPT through adsorption and redox at different initial concentrations.

According to the influence of temperature (298, 308, 318, 328 and 338K) on metal ions adsorption, the thermodynamic parameters (Gibbs free energy ( $\Delta G$ ), enthalpy ( $\Delta H$ ), and entropy ( $\Delta S$ ) can be determined using the following equations:

$$\ln K = \frac{-\Delta H}{RT} + \frac{\Delta S}{R} \quad (1)$$

$$\Delta G = \Delta H - T\Delta S \quad (2)$$

where,  $K (q_e/C_e)$  is the distribution coefficient under adsorption equilibrium.  $\Delta H$  and  $\Delta S$  can be calculated from a plot of  $\ln K$  versus  $1/T$  (Fig. S7). The positive values of  $\Delta H$  (3.17  $\text{kJ}\cdot\text{mol}^{-1}$ ) and  $\Delta S$  (18.60  $\text{J}\cdot\text{mol}^{-1}\cdot\text{K}^{-1}$ ) suggested that the adsorption of Cu(II) on MnPT increased the degree of disorder and that it was an endothermic process. Meanwhile, the positive values of  $\Delta H$  (13.41  $\text{kJ}\cdot\text{mol}^{-1}$ ) and  $\Delta S$  (72.48  $\text{J}\cdot\text{mol}^{-1}\cdot\text{K}^{-1}$ ) suggested that the adsorption of Cr(VI) on MnPT increased the degree of disorder and that it is an endothermic process. The negative value of  $\Delta G$  confirmed that this adsorption was spontaneous and feasible.

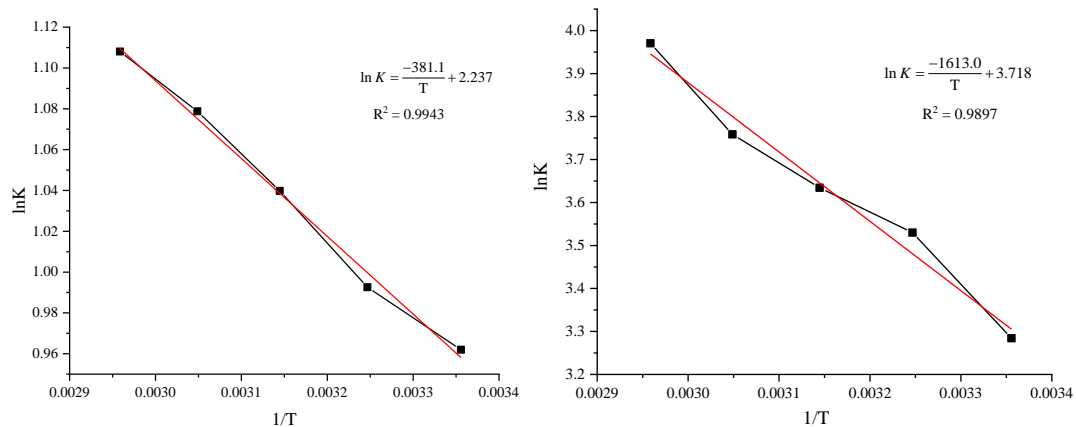


Fig.S7 The plot of  $\ln K$  versus  $1/T$  (a)Cu(II) adsorption (b)Cr(VI) adsorption

Fig. S8 presented the linear fitting results of the kinetic data of Cu (II) and Cr (VI) ions removal by MnPT. Fig. S5a and Fig. S8b presented the pseudo first order curves of Cu(II) and Cr(VI) adsorption. The inset in Fig. S5b presented the simulated curves for the initial 60 min of the adsorption process of Cr(VI). As seen the inset in Fig. S8b, the pseudo-first-order model worked well only for the first one hours of the Cr (VI) adsorption process. This indicated that there were many adsorption sites on the surface of MnPT at the beginning of adsorption and the pseudo-first-order model might not be sufficient to elucidate the mechanism of heavy metal adsorption. Fig. S8c and Fig. S8d presented the pseudo-second-order kinetic curves of Cu(II) and Cr(VI), respectively.

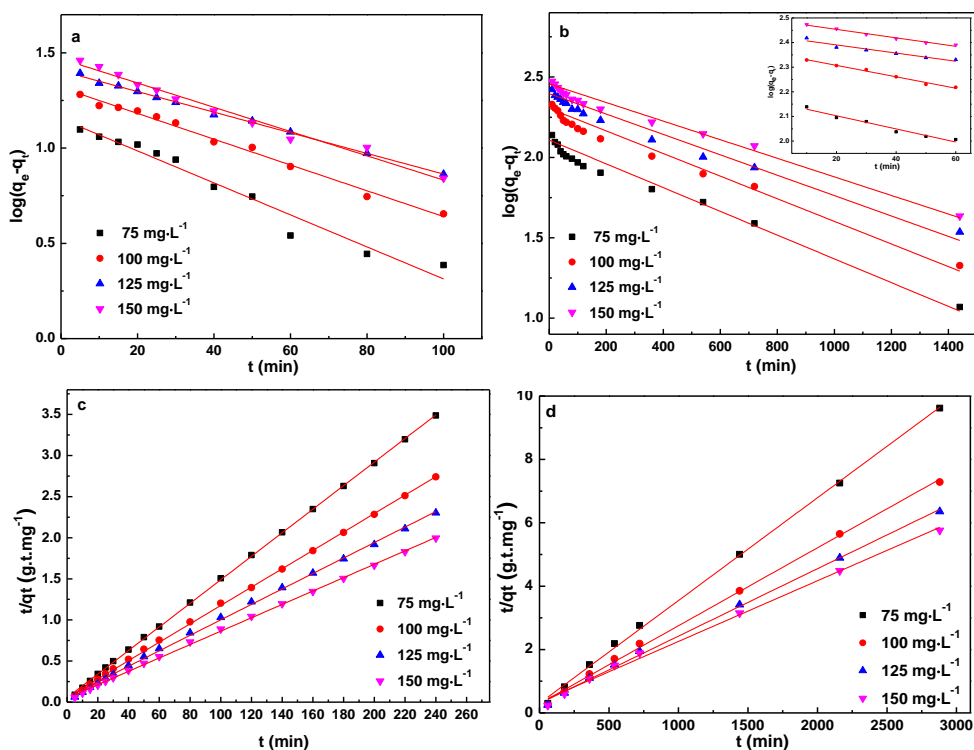


Fig. S8. Pseudo-first-order kinetics (a) and pseudo second-order kinetics (c) for Cu(II) adsorption on MnPT ( $T = 298$  K; pH = 5.5;  $C_0 = 75\text{--}150$  mg·L<sup>-1</sup>; MnPT = 100 mg·L<sup>-1</sup>; contact time = 4 h). Pseudo-first-order kinetics (b) and pseudo second-order kinetics (d) for Cr (VI) adsorption on MnPT ( $T = 298$ K; pH = 2.0;  $C_0 = 75\text{--}150$  mg·L<sup>-1</sup>; MnPT = 25 mg·L<sup>-1</sup>; contact time = 48 h).

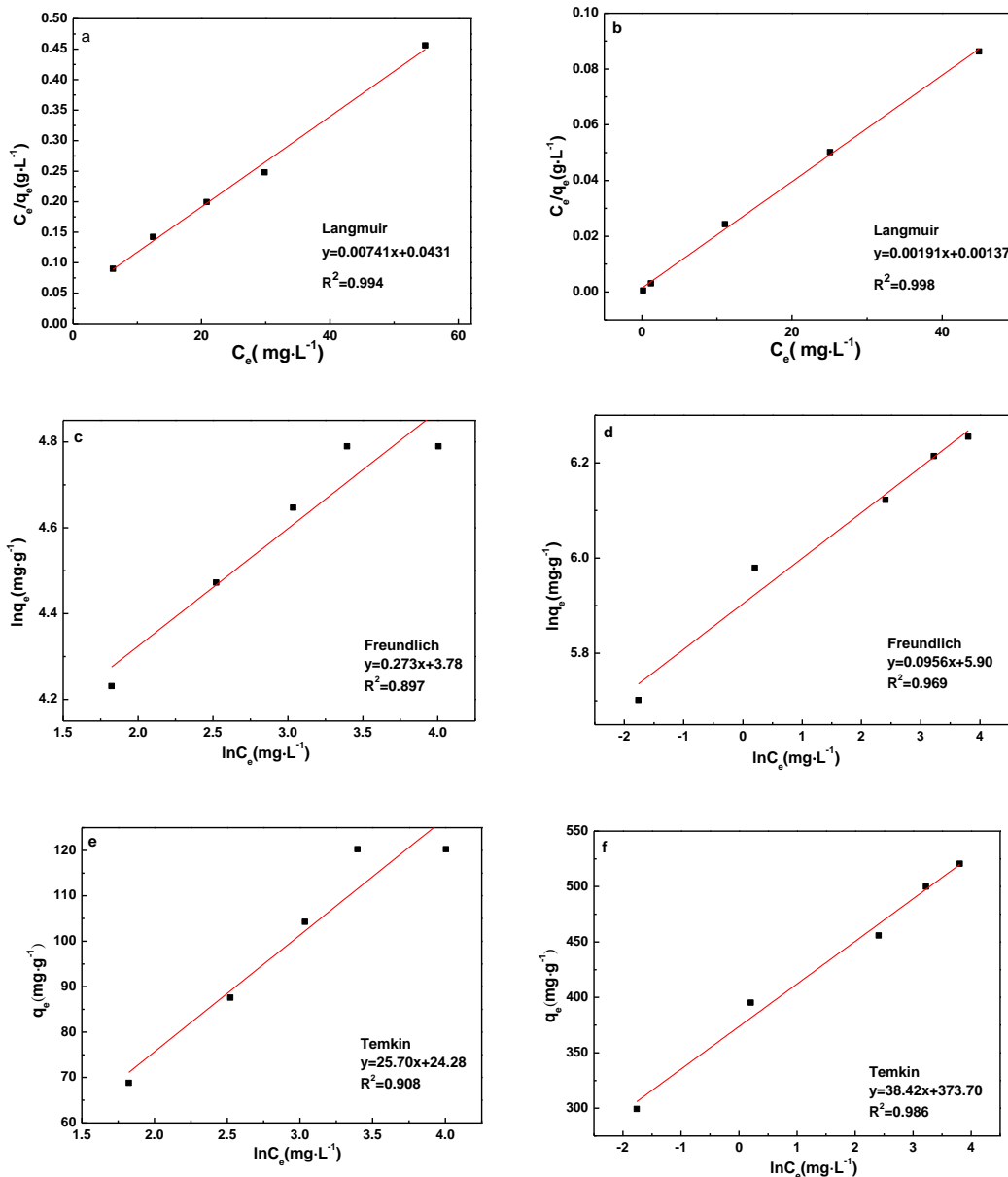


Fig. S9 (a) Langmuir isotherm, (c) Freundlich isotherm, and (e) Temkin isotherm plots for Cu(II) adsorption on MnPT ( $T = 298$  K; pH = 5.5;  $C_0 = 75\text{-}175$  mg L<sup>-1</sup>; MnPT = 100 mg L<sup>-1</sup>; contact time = 4 h). (b) Langmuir isotherm, (d) Freundlich isotherm, and (f) Temkin isotherm plots for Cr (VI) adsorption on MnPT ( $T = 298$ K; pH = 2.0;  $C_0 = 75\text{-}175$  mg L<sup>-1</sup>; MnPT = 25 mg L<sup>-1</sup>; contact time = 48 h).

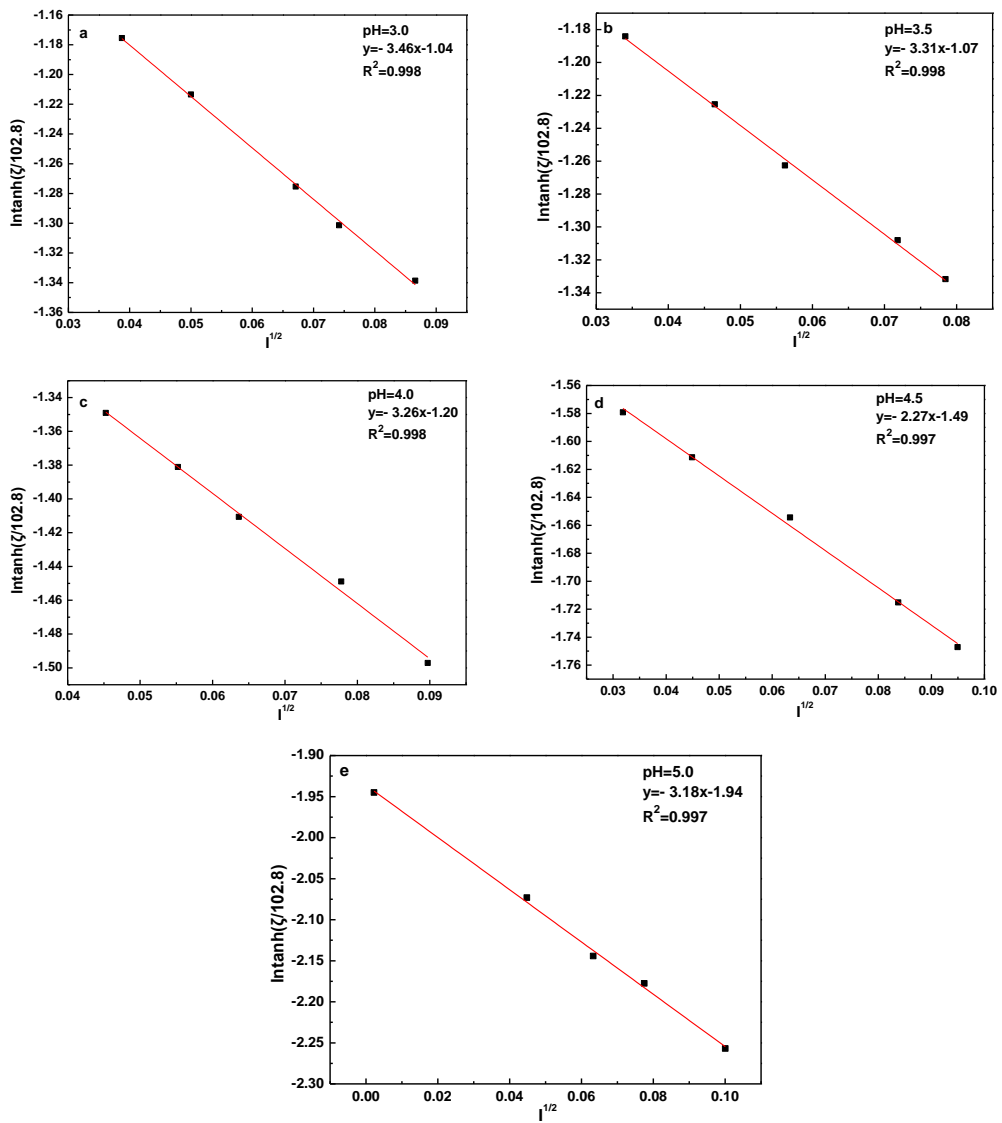


Fig. S10. Plots of  $\ln \tanh\left(\frac{\zeta}{102.8}\right)$  as a function of  $\sqrt{I}$  for MnPT particles in  $\text{NaNO}_3$  electrolyte. (a) pH = 3.0; (b) pH = 3.5; (c) pH = 4.0; (d) pH = 4.5; (e) pH = 5.0.

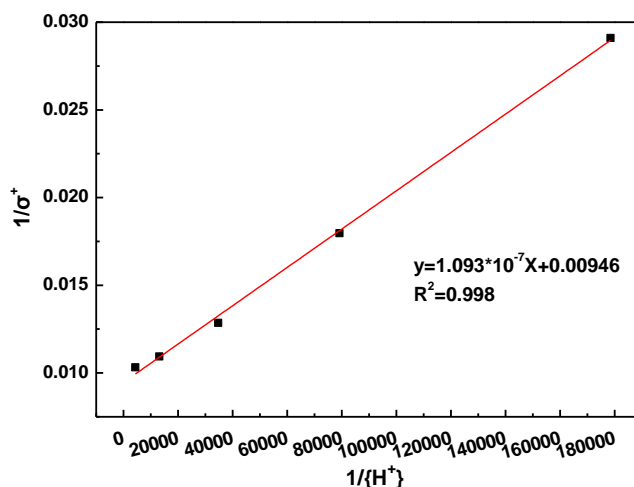


Fig. S11. Regression plot for determining surface acidity.

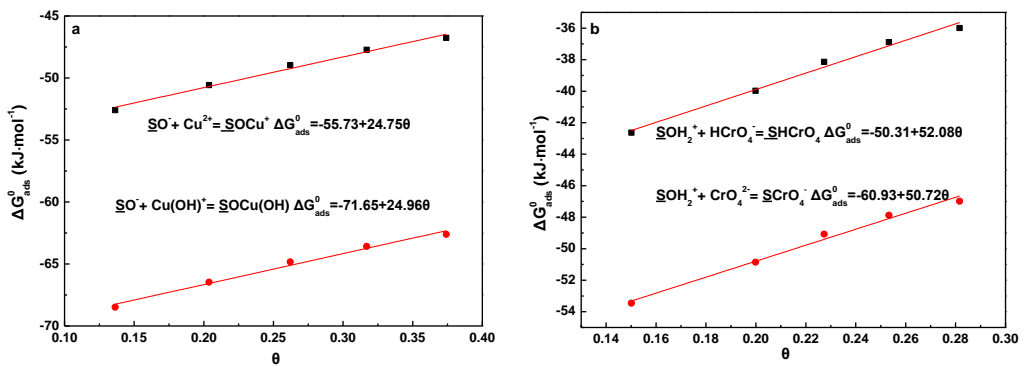


Fig. S12. (a) Adsorption energy for surface complexes  $\text{SOCu}^+$  and  $\text{SOCu}(\text{OH})$ , each as a function of surface coverage ( $\theta$ ); (b)

Adsorption energy for surface complexes  $\text{SOHCrO}_4$  and  $\text{SCrO}_4^-$ , each as a function of surface coverage ( $\theta$ );  $\theta$  was calculated from mass of Cu(II) or Cr(VI) adsorbed divided by total sites available for adsorption.

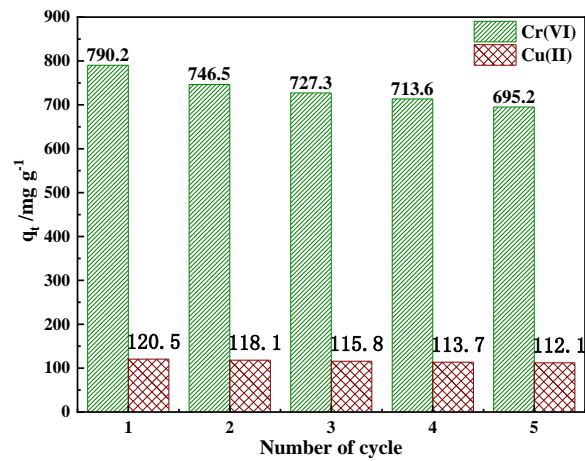
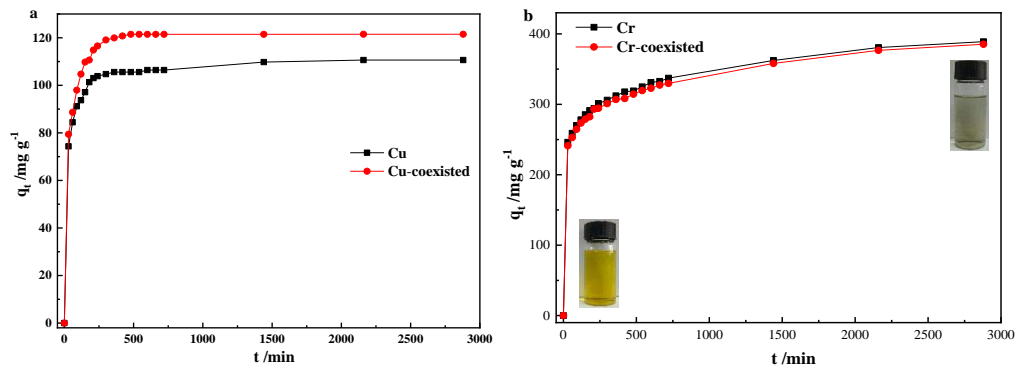


Fig. S13 Recycling five times for Cu(II) and Cr(VI) removal.